Macromolecules

pubs.acs.org/Macromolecules Article

# Spatial and Temporal Control of Photomediated Disulfide−Ene and Thiol−Ene Chemistries for Two-Stage Polymerizations

Shafer M. Soars,[⊥] Nicholas J. Bongiardina,[⊥] Benjamin D. Fairbanks, Maciej Podgórski, and Christopher N. Bowman*

Cite This: *Macromolecules* 2022, 55, 1811−1821 Read Online

ACCESS | Metrics & More | Article Recommendations | Supporting Information

**ABSTRACT:** A new strategy is reported for the design and synthesis of high sulfur-containing materials for potential use in covalent adaptable networks and optical materials by combining photomediated thiol−ene- and disulfide−ene-based polymerization reactions. Taking advantage of the relative reaction rates to differentiate sequentially between the thiol−ene and disulfide−ene conjugations, these reactions were performed semiorthogonally to produce polymer networks of controlled architecture. Kinetic analysis demonstrates that the thiol−ene reaction is approximately 30 times faster than the disulfide−ene reaction, enabling spatial and temporal manipulation of material properties *via* dual-cure networks and photopatterning. A two-stage polymerization approach was implemented with increases in modulus in the second stage of 2−3 orders of magnitude accompanied by increases in the glass-transition temperature of more than 15 °C. Additionally, the thiol−ene reaction in the presence of a disulfide yields materials capable of simultaneous network development and stress relaxation through dynamic bond exchange during *in situ* polymerization.

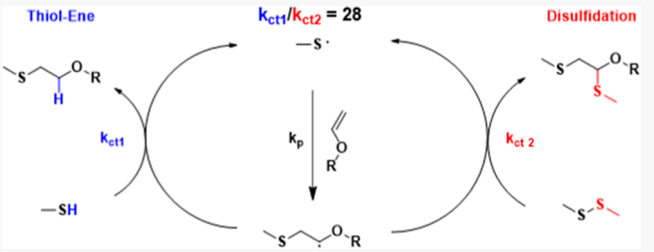


## INTRODUCTION

Over the last 50 years, sulfur-based chemistries have been widely applied to the field of polymer science and related applications.[1−4] Many of these chemistries involve thiol−X "click reactions" due to the high selectivity, rapid rates, and tolerability to various reaction conditions.[5−10] Other widely utilized sulfur-containing bonds include polysulfides which have been employed in the vulcanization of rubbers since the 19th century.[11−14]

The disulfide bonds, in particular, are intriguing covalent bonds that have been well studied in the literature, especially due to their crucial role in protein stability.[15] Although the disulfide bond is relatively strong (with a bond dissociation energy of roughly 60 kcal/mol), many disulfides are susceptible to cleavage by electrophiles, nucleophiles, reducing agents, free radicals, and even directly by specific wavelengths of light.[16−20] The unique chemistry surrounding disulfides has resulted in a recent surge of the incorporation of disulfides into polymeric systems. Polymers containing disulfides have been used for: stress relaxation, self-healing adaptable networks, controlled drug release, chain-transfer agents, increase of refractive index through the introduction of sulfur atoms, latent protection of thiols, and ring-opening polymerizations of 1,2-dithiolanes and 1,2-dithianes.[14,20−31]

The disulfidation of alkenes utilizing linear disulfides has generally been accomplished with transition-metal catalysis, limiting its utility in polymeric systems.[32−35] However, Bowman and co-workers recently reported the photo-induced radical-mediated disulfidation of vinyl ethers with various linear disulfides (Scheme 1a). The mechanism of this reaction parallels that of the thiol−ene/yne reactions (Scheme 1b), yielding thioacetal products in analogy to the thiol−yne bis thioether reaction products (Scheme 1c), providing 100%

**Scheme 1. Radical Conjugation Reactions Between Unsaturated Carbon−Carbon Bonds and Thiols or Disulfides in the Presence of an Initiator: (a) Disulfidation of Vinyl Ethers, (b) Thiol−Ene Reaction, and (c) Thiol−Yne Reaction**

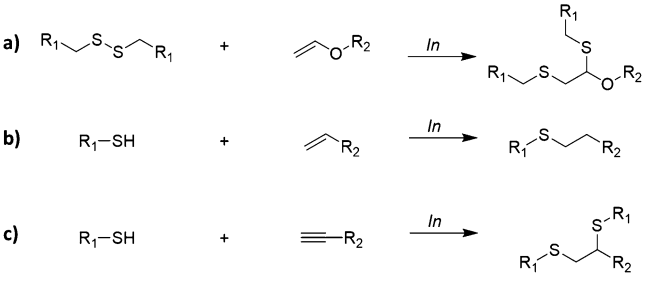


**Received:** November 30, 2021
**Revised:** January 24, 2022
**Published:** February 14, 2022

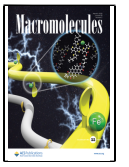







https://doi.org/10.1021/acs.macromol.1c02464
*Macromolecules* 2022, 55, 1811−1821

atom economy and overall pseudo-first-order kinetics with respect to the disulfide. Although the reactions are similar, it was demonstrated that the thiol−ene reaction exhibits a significantly faster reaction rate as compared to the disulfide−ene reaction.[36]

Furthermore, it was hypothesized that combining the thiol−ene and disulfide−ene reactions in a polymeric system (Scheme 2) would enable dual-cure (or two-stage) polymerization systems with spatial and temporal control over material properties. This approach would also enable dynamic covalent bond exchange, due to the inherent disulfide exchange mechanisms, as is necessary for covalent adaptable networks (CANs).[20] This work focused on a monomer containing a linear disulfide flanked with vinyl ethers (DSDVE), enabling polymerization of the monomer with multifunctional thiols *via* the radical-mediated thiol−ene reaction and subsequent disulfidation of the alkenes (Figure 1).

**Scheme 2. Schematic of the Competing Thiol−Ene and Disulfide−Ene Reactions Utilized in This Paper**

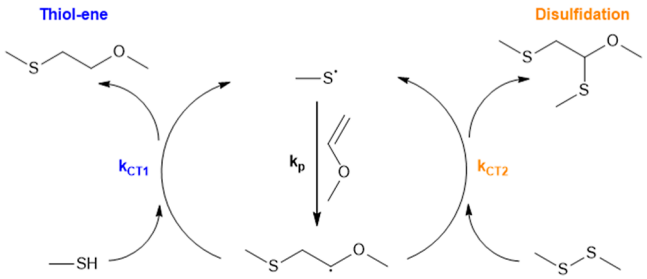


The disulfide monomer DSDVE was designed to enable several key characteristics of the linear disulfidation reaction. The molecule contains a dithioglycolate core, which has been previously shown to be the most effective functional group for the disulfidation reaction, achieving fast reaction rates and high overall yields. Although a dithioglycolate core is utilized, it is expected that other disulfides could be incorporated into this system to result in similar networks, albeit likely slower rates and lower conversions. Additionally, the pendent vinyl ether groups are vital because only vinyl ethers were shown to react on reasonable timescales in this disulfidation reaction scheme. Vinyl ethers also show excellent reactivity in the thiol−ene reaction. Finally, the butyl chains were incorporated such that the monomer would both be a liquid and miscible with the other components used herein.[36]

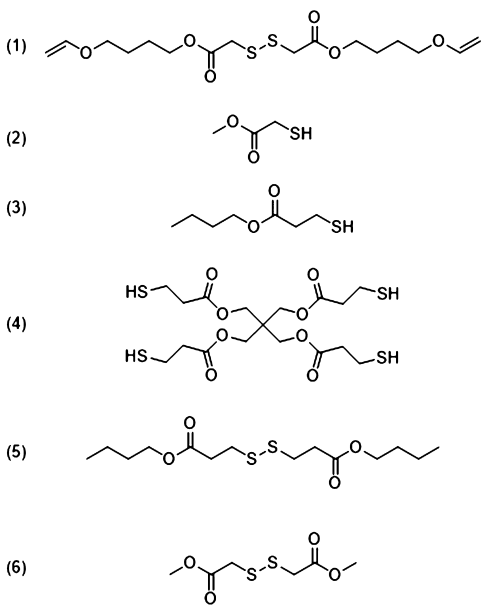


**Figure 1.** Materials used: (1) *bis*(butylvinylether) 2,2′-dithiodiglycolate (DSDVE). (2) Methyl thioglycolate (MTG). (3) Butyl-3-mercaptopropionate (BMP). (4) Pentaerythritol tetrakis(3-mercaptopropionate) (PETMP). (5) *Bis*(butyl) 3,3′-dithiobispropionate (DSMP). (6) *Bis*(methyl) 2,2′-dithioacetate (DSMA).

## MATERIALS

Dithioldiglycolic acid, diisopropylcarbodiimide (DIC), 4-dimethylaminopyridine (DMAP), methylthioglycolate (MTG), butyl-3-mercaptopropionate (BMP), pentaerythritol tetrakis(3-mercaptopropionate) (PETMP), 1,4-butanediol divinyl ether, diphenyl(2,4,6-trimethylbenzoyl)phosphine oxide (TPO), and anhydrous tetrahydrofuran (THF) were all purchased from Sigma-Aldrich. *Bis*(butylvinylether)dithiodiglycolate was synthesized as reported in the Supporting Information (Figure S1). All other chemicals were of reagent grade and used without further purification.

## EXPERIMENTAL SECTION

$^1$H-NMR and $^{13}$C-NMR spectra were recorded on a Bruker 400 MHz NMR spectrometer. Proton chemical shifts are expressed in parts per million ($\delta$). The $\delta$ scale was referenced to deuterated solvents, as indicated in the respective measurements.

**Real-Time Fourier Transform Infrared Spectroscopy.** Reaction kinetics were analyzed using a Fourier transform infrared (FTIR) spectrometer (Nicolet 8700) in transmission mode to monitor real-time functional group conversions. Samples were interposed between two NaCl windows and placed into a vertical transmission apparatus. Irradiation was performed using a mercury lamp (Acticure 4000) with a 400−500 nm band gap filter. The light intensity was measured by a THORLABS model number PM100D radiometer. By measuring the IR peak area decreasing at 1580−1670 and 2520−2620 cm$^{-1}$, the real-time functional group conversions of vinyl and thiol groups, respectively, were monitored and calculated as the ratio of the real-time peak area to the peak area of the initial spectra. The alkene peak was also verified by additionally measuring the IR peak area decreasing at 790−850 cm$^{-1}$.

**Rheometry.** Data were collected using Ares G2 (TA Instruments) with a 20 mm plate at 25 °C with a 0.5% strain at a frequency of 1 Hz using a photo-rheometry attachment connected to an Acticure light source. Samples were irradiated *in situ*, and the loss and storage moduli were monitored.

**Dynamic Mechanical Analysis.** Dynamic mechanical analysis (DMA) was performed on an RSA-G2 system (TA Instruments). Samples of approximate dimensions 20 mm × 5 mm × 0.25 mm ($L \times W \times H$) were cut, and measurements were taken using a temperature ramp rate of 3 °C/min at a frequency of 1 Hz to measure the storage modulus, loss modulus, and tan($\delta$). The glass-transition temperature ($T_g$) was taken to be the peak of tan($\delta$) of the second temperature ramp of two temperature sweeps.

## RESULTS AND DISCUSSION

**Kinetics.** A thorough kinetic analysis was conducted to gain a better understanding of the disulfidation and thiol−ene disulfidation polymerizations. Fundamental kinetic parameters were determined by experiments with monofunctional model compounds to avoid confounding variables (*e.g.*, decreasing reactant mobility) that may complicate the analysis of the kinetics during the polymerization and cross-linking reactions. Initial studies were conducted to obtain the first estimate of the chain-transfer kinetic constant for the disulfidation reaction


https://doi.org/10.1021/acs.macromol.1c02464
Macromolecules 2022, 55, 1811−1821

involving only the disulfide−diene monomer. Subsequently, DSDVE was mixed and reacted with MTG at various stoichiometric ratios to obtain kinetic constants for both possible chain-transfer reactions and to ascertain how fast the thiol−ene reaction is relative to disulfidation when there is only one possible thiyl radical. Finally, DSDVE was reacted with BMP to examine the relative kinetics where a potential mixture of two types of thiyl radicals could exist. BMP was selected as a monofunctional analogue of PETMP, a common multifunctional thiol used in thiol−ene polymerizations.

**Kinetics of the Disulfidation of DSDVE.** A detailed kinetic analysis of the thiol−ene disulfidation polymerizations is crucial to controlling the material properties in a polymer network. The first step toward the understanding of the evolution of the thiol−disulfide−ene networks is to evaluate the kinetics of the disulfidation polymerization of DSDVE independent of the thiol−ene reaction. We propose a model for the kinetics of the disulfidation reaction derived directly from the thiol−ene kinetics. Here, the thiols in the thiol−ene equations are replaced with disulfides because they play an analogous role to the thiol in both the propagation and chain-transfer steps.[37] Based on the mechanism in Scheme 2, the governing equations (eqs 1−4) used to model the disulfidation kinetics are as follows.

$$\frac{d[C=C]}{dt} = -k_p[C=C][S^\bullet] \quad (1)$$

$$\frac{d[S-S]}{dt} = -k_{ct}[S-S][C^\bullet] \quad (2)$$

$$\frac{d[S^\bullet]}{dt} = R_i - R_t(S^\bullet) + k_{ct}[S-S][C^\bullet] - k_p[C=C][S^\bullet] \quad (3)$$

$$\frac{d[C^\bullet]}{dt} = -R_t(C^\bullet) - k_{ct}[S-S][C^\bullet] + k_p[C=C][S^\bullet] \quad (4)$$

Equation 1 accounts for the concentration of the alkenes (vinyl ethers), which are consumed by the propagation of a thiyl radical through a double bond. Equation 2 accounts for the concentration of disulfides, which react *via* the chain transfer of a carbon-centered radical to the disulfide. Equations 3 and 4 describe the concentration of the thiyl and carbon-centered radicals, respectively, considering the initiation, termination, propagation, and chain-transfer events for both radical species.

The initiation and termination rates are predicted by eqs 5−7.[37] Equation 5 is the rate of initiation ($R_i$, M/s), where standard values for TPO were used ($f$ = initiator efficiency (0.2), $\varepsilon$ = molar absorption [230 L/(mol•cm)],[38] [I] = initiator concentration, $I_0$ = light intensity, $\lambda$ = wavelength (405 nm), NA = Avogadro's number, $h$ = Planck's constant, and $c$ = speed of light in a vacuum). Equations 6 and 7 account for the rates of termination for the carbon and thiyl radicals, respectively. For simplicity, all bimolecular termination pathways are considered to be equally likely; therefore, $k_t$ (1,000,000 $M^{-1}•s^{-1}$) is assumed to be the same for each termination pathway.[37] This system of seven equations was solved numerically to model the concentration of the disulfide and alkene over time and compare the theoretical alkene concentration to experimental data. Although an analytical solution is possible for this simple set of equations given a few assumptions (*i.e.*, pseudo-steady-state radical concentration and equal rates of functional group consumption),[9,37] numerical solutions using the ode45 function in MATLAB were implemented for consistency with the subsequent modeling of the combined thiol−ene disulfidation reaction scheme.

$$R_i = \frac{(2.303f \in [I]I_0\lambda)}{(N_A hc)} = k_i[I] \quad (5)$$

$$R_t(C^\cdot) = 2k_t[C^\cdot]^2 + k_t[C^\cdot][S^\cdot] \quad (6)$$

$$R_t(S^\cdot) = 2k_t[S^\cdot]^2 + k_t[C^\cdot][S^\cdot] \quad (7)$$

The conversion of the alkene during the disulfidation polymerization of DSDVE was measured *via* FTIR and is provided in Figure 2. The reaction was performed with 1.5 wt

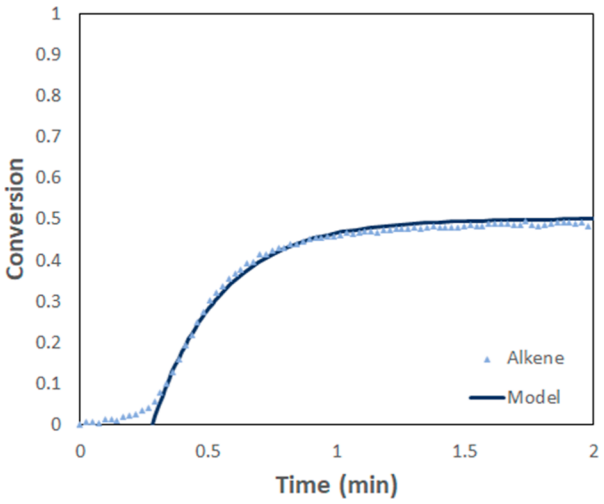


**Figure 2.** Kinetics of the disulfidation reaction of DSDVE and the model kinetics. The reaction reaches full conversion of disulfide and 50% conversion of alkene due to the off-stoichiometric ratio of the reactants (2:1 ratio of alkene/disulfide). The reaction contained 1.5 wt % TPO which reacted with 14 mW/cm$^2$ of light at 405 nm. Full conversion is achieved after roughly 1 min of irradiation time.

% TPO as a photoinitiator and was activated with 405 nm light at 14 mW/cm$^2$ light intensity. The inherent stoichiometry of this reaction is a 1:2 disulfide to alkene due to the disulfide core with two flanking vinyl ether groups. Therefore, the theoretical conversion of the alkene is 50% if every disulfide is consumed during the polymerization. There is a clear induction period during the early stage of this reaction that is attributed to oxygen inhibition.[36] Upon overcoming this inhibition, the reaction proceeds, and the alkene indeed reaches approximately 50% conversion, which is assumed to correspond to the complete consumption of the disulfide. The numerical model was fit to the experimental best fit value after oxygen inhibition has been overcome with $k_{ct}$ of 8000 $s^{-1}$. When the reaction is chain-transfer-limited, as it appears here, $k_p$ is necessarily much larger than $k_{ct}$, and its specific value does not alter the overall reaction rate significantly. Propagation kinetic constants for thiol−ene reactions in the literature between thiols and vinyl ethers are reported to be near that of chain transfer ($k_p/k_{ct}$ = 1.2), with $k_p$ on the order of 130,000 $s^{-1}$ for 3-mercaptopropionate under conditions similar to those implemented here, indicating a much faster reaction than that between the disulfide and vinyl ether. As the propagation


https://doi.org/10.1021/acs.macromol.1c02464
Macromolecules 2022, 55, 1811−1821

Scheme 3. Competing Reactions of a Vinyl Ether Between the Thiol−Ene and Disulfide−Ene Reactions

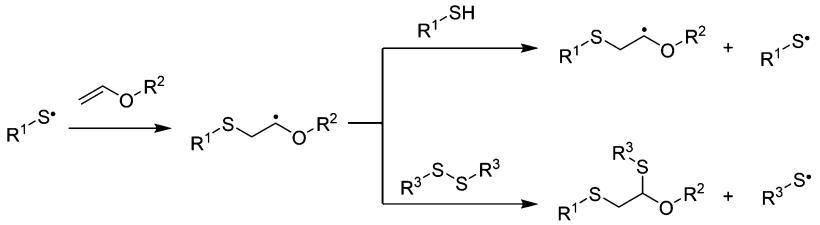

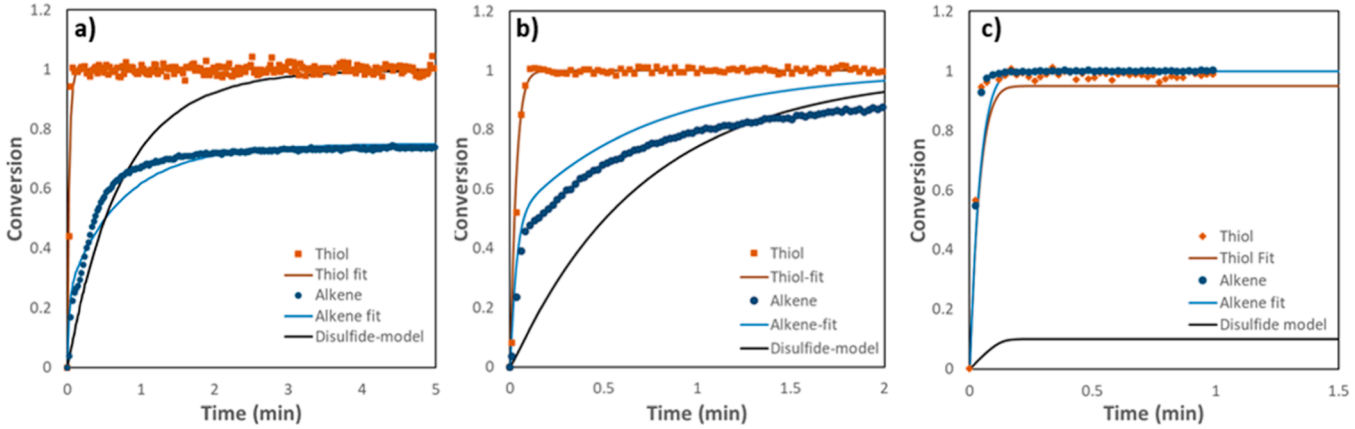


**Figure 3.** Conversion over time for the thiol and alkene for DSDVE and MTG with the overall model fits ($k_p$ = 164,000 $s^{-1}$, $k_{ct1}$ = 136,000 $s^{-1}$, and $k_{ct2}$ = 4800 $s^{-1}$), as well as the predicted disulfide conversion for (a) 0.25:1 ratio of thiol to alkene, (b) 0.5:1 ratio of thiol to alkene, and (c) 1:1 ratio of thiol to alkene. Reactions contained 0.5 wt % TPO and were initiated by 7 mW/$cm^2$ light at 405 nm.

reaction between the thiyl radical and the vinyl ether should be similar, regardless of whether the thiyl radical is generated from a thiol or a disulfide, this literature value of $k_p$ = 130,000 $s^{-1}$ was used to calculate an estimate for $k_p/k_{ct}$ for the disulfidation of DSDVE of 16.

**Methyl Thioglycolate: Thiol−Ene Disulfidation Kinetics.** Introducing thiol into this reaction scheme results in two competing reaction pathways, namely the thiol−ene and disulfide−ene reactions, that share a propagation step in which the thiyl radical adds into an alkene to generate a carbon-centered radical. The chain-transfer step may then proceed to either the thiol−ene reaction, by abstracting a hydrogen from a thiol, or through the disulfidation reaction by reacting with and cleaving the disulfide (Scheme 3). The more prevalent pathway at a given point in time therefore depends on both the relative chain-transfer rate constants and the concentrations of thiol and disulfide.

The propagating carbon radical chain transfers to a thiol or a disulfide to yield distinct products.

Competition between these reactions was analyzed by exploring the reaction between MTG and DSDVE. Regardless of whether chain transfer occurs with a thiol or a disulfide, the reaction of either MTG or DSDVE results in a thioglycolate radical. Thus, this parallel reaction enables kinetic analysis that includes only a single type of thiyl radical. In addition to the thiol−ene reaction, the introduction of thiol to this scheme also enables the radical−disulfide exchange between the thiol and the disulfide during the thiol−ene stage of the reaction. This pathway is not directly accounted for in the kinetic model, as the initial and final species are chemically identical, but is implicitly accounted for within the chain-transfer step for thiol−ene because the product of the radical disulfide exchange reaction does not change the kind of thiyl radicals that are present in the reaction.

A model that also takes the thiol−ene pathway into account is presented in the species mass balances presented in eqs 8−12. The new terms introduced for the thiol−ene disulfidation model are colored blue for additional clarity. Equation 8 accounts for the thiol concentration by the chain transfer of the carbon-centered radical to the thiol. Equation 9 describes the alkene consumption and is identical to eq 1 because both thiol−ene and disulfide−ene share the same propagation step. Equation 10 describes the disulfide consumption and is nearly identical to eq 2, where $k_{ct}$ has been replaced by $k_{ct2}$ to differentiate between the two different chain-transfer constants. Equations 11 and 12 account for the thiyl and carbon radicals, respectively, with terms that factor in chain transfer to a thiol ($k_{ct1}$) and chain transfer to a disulfide ($k_{ct2}$). Because radical disulfide exchange is possible during the thiol−ene step of the reaction, the $k_{ct1}[SH][C^•]$ term represents the net chain transfer rate after any disulfide exchange event occurs. This system of equations was then solved numerically using the ode45 function in MATLAB and fit to experimental data.

MTG was used in a model study at three different stoichiometries of thiol-to-alkene: 0.25:1, 0.5:1, and 1:1. These stoichiometries were selected to demonstrate a robust kinetic model at different thiol, disulfide, and alkene concentrations. Mild initiation conditions, 0.5 wt % TPO photoinitiator and 7 mW/$cm^2$ of 405 nm light, were used to slow down the reaction, such that any differences in rate could be more easily distinguished and accurately measured. For all three stoichiometries, the ratio of propagation to chain-transfer kinetic constants for the thiol−ene reaction ($k_p/k_{ct1}$) of 1.2 was used as a previously calculated value from the literature (Cramer *et al.*).[37] Therefore, the model was fit to the data by adjusting only the ratio of the thiol−ene and disulfidation chain-transfer kinetic constants ($k_{ct1}/k_{ct2}$).



https://doi.org/10.1021/acs.macromol.1c02464
Macromolecules 2022, 55, 1811−1821

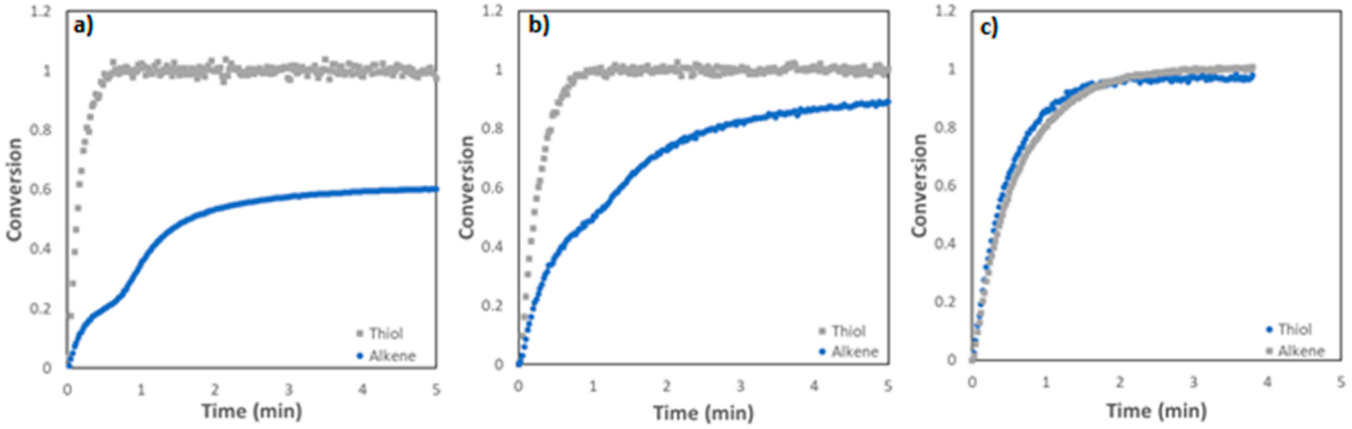


**Figure 4.** Conversion over time for the thiol and alkene for DSDVE with BMP: (a) 0.25:1 ratio of thiol to alkene, (b) 0.5:1 ratio of thiol to alkene, and (c) 1:1 ratio of thiol to alkene. Reactions contained 0.5 wt % TPO, 14 mW/cm$^2$ at 405 nm.

$$\frac{d[SH]}{dt} = -k_{ct1}[SH][C^\bullet] \quad (8)$$

$$\frac{d[C=C]}{dt} = -k_p[C=C][S^\bullet] \quad (9)$$

$$\frac{d[S{-}S]}{dt} = -k_{ct2}[S{-}S][C^\bullet] \quad (10)$$

$$\frac{d[S^\bullet]}{dt} = R_i - R_t(S^\bullet) + k_{ct1}[SH][C^\bullet] + k_{ct2}[S{-}S][C^\bullet] - k_p[C=C][S^\bullet] \quad (11)$$

$$\frac{d[C^\bullet]}{dt} = -R_t(C^\bullet) - k_{ct1}[SH][C^\bullet] - k_{ct2}[S{-}S][C^\bullet] + k_p[C=C][S^\bullet] \quad (12)$$

Representative FTIR data for the thiol and alkene conversion over time for all three stoichiometries and the model fit are shown in Figure 3. A single set of kinetic parameters was used to fit all three stoichiometries, where $k_{ct1}$ = 136,000 s$^{-1}$ and $k_{ct2}$ = 4800 s$^{-1}$, which results in $k_{ct1}/k_{ct2}$ = 28. The conversion over time and model fits for the 0.25:1 ratio of thiol to alkene are provided in Figure 3a. Under these reaction conditions, there is no adequate disulfide peak in the infrared spectrum, so the conversion as a function of time, as predicted by the model, is shown. At this stoichiometry, there are sufficient thiols and disulfides to react with a total of 75% of vinyl ethers, with 25% conversion attributed to the thiol−ene reaction and 50% conversion attributed to disulfidation. As predicted, a rapid thiol−ene reaction is observed within the first few seconds, followed by a slower disulfidation step, with the transition from the thiol−ene to the disulfide−ene reaction occurring at roughly 25% conversion of the alkene, as dictated by the reaction stoichiometry. The discrepancies in the measured rate of chain transfer between the disulfide and the carbon radical in the absence or presence of the thiol−ene reaction is largely attributed to the decrease in mobility (*i.e.*, viscosity), as well as changes in other aspects such as polarity. The model slightly underpredicts the rate of disulfide exchange but accurately predicts the thiol−ene rate and the overall conversion of the reaction.

Next, representative FTIR data for the thiol and alkene conversion and model prediction for the 0.5:1 ratio of thiol to alkene are provided in Figure 3b. Here, all functional groups should be consumed once both the thiol−ene and disulfidation reactions are complete, with a transition occurring around 50% conversion of the alkene. Once again, two regimes are indeed observed: an initial rapid thiol−ene step, followed by a slower disulfidation step which occurs after about 50% conversion, as predicted. Once again, the model accurately predicts the rate of the thiol−ene reaction, but this time it overpredicts the rate of the disulfide reaction by missing the short "ramp-up" period between the two reaction mechanisms.

Representative FTIR data for thiol and alkene conversions for the 1:1 ratio of thiol to alkene are provided in Figure 3c with their corresponding model fits. Here, only the thiol−ene reaction should occur, rapidly consuming all of the alkenes before the disulfides have a chance to react. Indeed, a single rapid reaction is observed, with 1−2% of the thiol left unreacted due to the minimal conversion of the disulfides. A separate disulfidation step does not occur because nearly all of the alkenes are consumed by the thiols. In this case, the model slightly underpredicts the rate of the thiol−ene reaction relative to disulfidation by overpredicting the amount of unreacted thiol (by 2−3% conversion) due to the alkene consumption by the disulfides that was observed in the data.

The kinetic model shows reasonably good agreement with the experimental data, and the thiol−ene reaction is approximately 30 times faster than the disulfidation reaction for this system. This rate difference is largely attributed to the fact that the hydrogen atom of a thiol is significantly more sterically accessible than the disulfide bond, resulting in the rapid extraction of the hydrogen atom from the thiol relative to the homolytic cleavage of the disulfide to regenerate a thiyl radical. Some discrepancies were observed across the stoichiometric ratios tested; however, the model performed well overall in predicting the rate and conversion across three different stoichiometric ratios. These small discrepancies are, in part, attributed to the fact that radical−disulfide exchange is not directly accounted for in this model, and differences in disulfide concentration can impact the rate differently for each stoichiometry tested. The contribution of radical−disulfide exchange for each stoichiometry will be different because the relative concentration of disulfide to thiol cannot be kept constant due to the fixed 2:1 alkene/disulfide stoichiometry imposed by the DSDVE monomer. Therefore, changing the thiol-to-alkene stoichiometry must also change the relative amount of disulfide and therefore the rate of the exchange. Directly accounting for radical−disulfide exchange would require the knowledge of the rate constants for the addition of the thiyl radical to the disulfide and the fragmentation of


https://doi.org/10.1021/acs.macromol.1c02464
*Macromolecules* 2022, 55, 1811−1821

Scheme 4. (a) Theoretical Mechanism of Radical Disulfide Exchange Between BMP Thiyl Radical and DSMA[a]

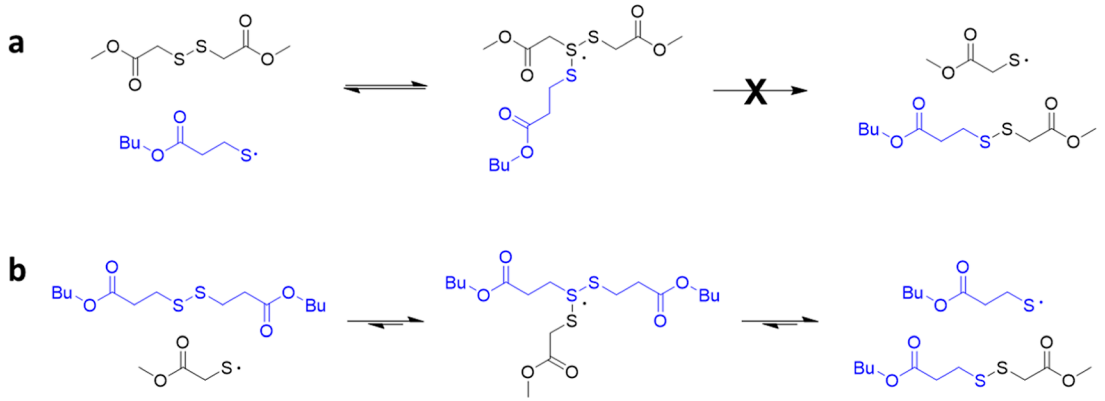

[a]Experimental reaction performed *via* a mixture of DSMA (1 equiv) and BMP (1 equiv) with 1.5 wt % TPO irradiated at 405 nm at 14 mW/cm$^2$. This reaction condition resulted in only the recovery of starting compounds as detected by $^1$H NMR. (b) Theoretical mechanism of radical disulfide exchange between MTG thiyl radical and DSMP. Experimental reaction performed *via* a mixture of DSMP (1 equiv) and MTG (1 equiv) with 1.5 wt % TPO irradiated at 405 nm at 14 mW/cm$^2$. This reaction condition resulted in a mixture of corresponding disulfides and thiols as detected by $^1$H NMR.

that intermediate back into the radical and disulfide. These rate constants are not, as of this paper, available in the literature except for a small set of purely aliphatic disulfides.[12,20,28] Additionally, the assumption of equal rates of all termination pathways also contributes to these discrepancies as changes in stoichiometric ratios will alter the concentration of the various radicals present in the polymerization and therefore which termination pathways predominate. Overall, this kinetic analysis shows that thiols and disulfides of the same type can co-react in a controlled manner with vinyl ethers.

**Butyl 3-Mercaptopropionate: Thiol−Ene Disulfidation Kinetics.** Implementing thiol−ene disulfidation polymerizations for practical applications will also involve frequently used multifunctional mercaptopropionate monomers in addition to thioglycolate-based monomers (such as PETMP), which have one additional carbon between the thiol and the carbonyl. It is therefore important to study the impact of introducing different thiyl radical species into the polymerization aside from the radicals formed by the disulfidation reaction on functional group conversions and reaction rate. This analysis is especially important because radical disulfide exchange is inherently possible during these radical polymerizations and the presence of a different thiol may impact the polymerization rate *via* one or both reactions. To study this impact directly, butyl 3-mercaptopropionate (BMP) was used with DSDVE to study any effects of mixed thiyl radicals on the reaction without the additional complexities of a polymerization reaction such as increases in viscosity and cross-linking.

This study was conducted at the same three stoichiometric ratios of thiol to alkene as BMP: 0.25:1 to reach 75% alkene conversion, 0.5:1 to consume all functional groups, and 1:1 such that essentially only the thiols appreciably react with the alkenes. The conversion over time for the thiol and alkene for each functional group ratio is provided in Figure 4a−c.

All three stoichiometric ratios show similarities and a key difference from the experiments conducted with MTG. Overall, the temporal separation of thiol−ene and disulfidation reactions are nearly identical in terms of the conversion at which the transition occurs. For the 0.25:1 and 0.5:1 ratios of thiol to alkene, there are distinct thiol−ene and disulfidation steps that transition at 25 and 50% alkene conversion, respectively. Likewise, the 1:1 stoichiometry shows only a thiol−ene reaction in which there is a small amount of residual, unreacted thiol due to a correspondingly small amount of disulfide consumption. However, in all three cases, the thiol−ene rate of polymerization for MTG is faster than that for BMP, where the transition to disulfidation occurs after a few seconds for MTG but nearly a minute for BMP. This result is counterintuitive because, in the context of this thiol−ene reaction, the mercaptopropionate radical formed during the thiol−ene reaction with BMP should have improved chain transfer compared to that with MTG, due to the weakening of the SH bond by intramolecular hydrogen bonding with the carbonyl in a favored six-membered ring arrangement.[39] This behavior was confirmed *via* FTIR experiments using BMP and MTG with triethylene glycol divinyl ether, a nondisulfide containing divinyl ether, for which BMP shows a faster thiol−ene reaction rate than MTG (Supporting Information Figure S3).

The explanation as to why BMP shows a slower rate of reaction than MTG in the presence of DSDVE centers on the radical disulfide exchange pathway that is expected to occur. Because the thiyl radical formed *via* chain transfer to BMP is different from that formed from the chain transfer to MTG and DSDVE, it is not immediately clear which products of radical disulfide exchange would predominate in this context, but it is clear that the additional complexity introduced by different thiyl radical species impacts the rate of the thiol−ene reaction, likely due to the tendency to form the lowest energy, least reactive thiyl radical. However, there was no discernible change in the disulfidation rate with BMP compared to that with MTG, indicating that any retardation process only impacts the thiol−ene step of the reaction. A possible explanation is that although the BMP thiyl radical adds into the disulfide to form a radical intermediate reducing the thiyl radical concentration, the original BMP radical and disulfide reform because of the enhanced stability of the BMP radical relative to an MTG radical.

This pathway would slow the thiol−ene step by temporarily sequestering thiyl radicals without converting any symmetric dithioglycolate disulfides to a mixture of symmetric and asymmetric disulfides, leaving the disulfidation step unaffected.



https://doi.org/10.1021/acs.macromol.1c02464
Macromolecules 2022, 55, 1811−1821

Furthermore, this proposed mechanism predicts that the radical intermediate formed by a BMP radical may have a longer lifetime than the intermediate formed by an MTG radical due to the additional electron density associated with the additional carbon atom between the sulfur and the carbonyl, which would sequester BMP radicals longer in this intermediate state than MTG radicals, specifically when DSDVE is the disulfide-containing monomer.

To investigate the cause of the change in thiol−ene rates, mixed disulfide−thiol NMR experiments were performed to probe whether the BMP radicals and dithioglycolate disulfides are in fact the favored products. Two thiol−disulfide mixtures were used in the presence of 1.5 wt % TPO photoinitiator. First, a mixture of DSMA and BMP was tested (Scheme 4a), which is analogous to that of DSDVE−BMP because it contains the same disulfide/thiol pair. No change in the peaks or peak integration was observed after 10 min of irradiation at 14 mW/cm$^2$ (Supporting Information Figures S4 and S5). This indicates that no significant amounts of new disulfides or thiols formed during the disulfide exchange process. To test this further, DSMP and MTG were mixed with the photoinitiator TPO and irradiated (Scheme 4b). This mixture is the complementary pair of thiol and disulfide, where the disulfide is based on BMP instead of MTG. Here, there is a clear appearance of new peaks after irradiation (Supporting Information Figures S6 and S7) due to the formation of BMP and a mixture of disulfides due to the radical thiol−disulfide exchange. These results suggest that the radical disulfide exchange does occur for these disulfides with BMP and that the BMP radical is in fact the more stable thiyl radical. Taken together, these results support the hypothesis that the thiol−ene step is slower with BMP than with MTG because the exchange pathway sequesters thiyl radicals to a greater extent for BMP without disulfide exchange. This lack of disulfide exchange in this system with BMP portends predictable architecture, whereas the disulfide exchange with MTG may result in asymmetric disulfides and less predictable polymer architectures. In an analogous hypothetical system with a mercaptopropionate disulfide core, it would be expected that polymer architecture is less predictable with both BMP- and MTG-based cross-linkers. Further investigation is ongoing to explore how this phenomenon could be used to tailor the polymer architecture.

**Gelation of DSDVE.** It was not immediately obvious if the polymerization of DSDVE would form a cross-linked network. A similar system based on a monomer containing a mono-thiol and mono-alkyne generates hyperbranched polymers;[40] however, polymerization of DSDVE does in fact yield an insoluble cross-linked network (Figure 5). Such an outcome could also be expected if some of the disulfides remained unreacted or the alkenes underwent a degree of homopolymerization, or both of these scenarios. However, the photoinitiated polymerization of DSDVE is difficult to be evaluated *via* the Flory−Stockmayer relationship due to the complexities that are unique to this polymerization, namely the requirement that both reaction sites on the alkene must react during a single polymerization cycle as compared to the thiol−yne reaction where a single site may react before the second. However, it can be conceptually simplified to a reaction between difunctional and trifunctional monomers with complementary functional groups in a 2:1 molecular ratio (Figure 6). In such a system, under ideal and uniform reaction progress, two difunctional monomers would react with one trifunctional

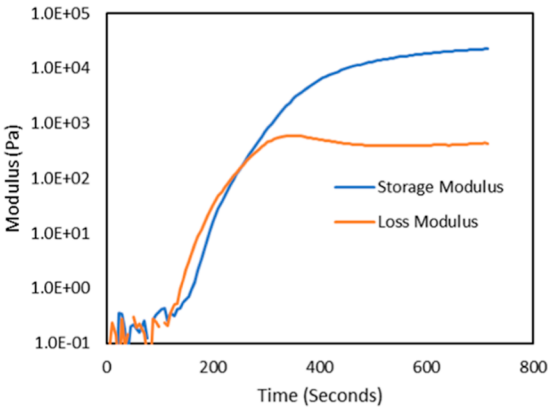


**Figure 5.** Rheometry data for the photopolymerization of DSDVE with 1.5 wt % TPO irradiated at 405 nm at 14 mW/cm$^2$. Data demonstrate cross-linking by the storage modulus crossing the loss modulus after roughly 2 min of light exposure.

complement to create a heterotrifunctional compound such as the one illustrated in Figure 6.

This hypothetical compound and arrangement of complementary bonds is equivalent to the fundamental reactive unit obtained by the radical cleavage of the disulfide, wherein the sulfur radical is monofunctional and the vinyl ether is difunctional. According to Flory−Stockmayer,[41] the critical conversion for gelation (the minimum conversion the limiting functional group must reach for network formation) is described by eq 13.

$$p_c = \frac{1}{[r(f_{w,A} - 1)(f_{w,B} - 1)]^{1/2}} \tag{13}$$

where $p_c$ is the critical conversion, $r$ is the stoichiometric imbalance defined as the moles of limiting functional group divided by the moles of excess complementary functional group, $f_{w,A}$ is the weight-averaged functionality of the designated "A" functional group monomers, and $f_{w,B}$ is the weight-averaged functionality of the designated "B" functional group monomers (3 and 2 in this case, respectively). The stoichiometric imbalance, in this case, would be 0.75 for the three A groups divided by the four B groups, resulting in a critical conversion of 0.82, well within the range of achievable extent of reaction. It should be noted that a similar hypothetical heterotrifunctional species can be obtained by reacting a single trifunctional A compound with a single difunctional B compound, in which case the stoichiometric imbalance would be 2/3 and the critical conversion would be 0.87, again below the limit of 1.0. The Carothers equation for gelation,[41] shown in eq 14, where $f_{avg}$ is defined simply as the total number of limiting functional groups divided by the total number of reactive species, yields a different result.

$$p_c = \frac{2}{f_{avg}} \tag{14}$$

By this equation, critical gelation conversion is calculated as that at or above the maximum possible conversion of 100%, indicating no gelation is possible. In practice, experimental gel point conversions frequently lie somewhere between these two simple and common predictive models. While the Flory-Stockmayer statistical treatment is typically preferred for gel point predictions, the results from the Carothers equation serve to demonstrate that this system is likely on the cusp of


https://doi.org/10.1021/acs.macromol.1c02464
Macromolecules 2022, 55, 1811−1821

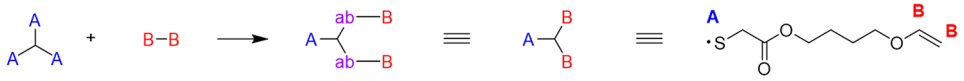


**Figure 6.** Schematic representation of the disulfide−ene reaction of DSDVE. This representation is a depiction of the fundamental reactive unit obtained after radical cleavage of the disulfide. "A" depicts a thiyl radical and the "B"s represent the alkene that acts as a difunctional unit.

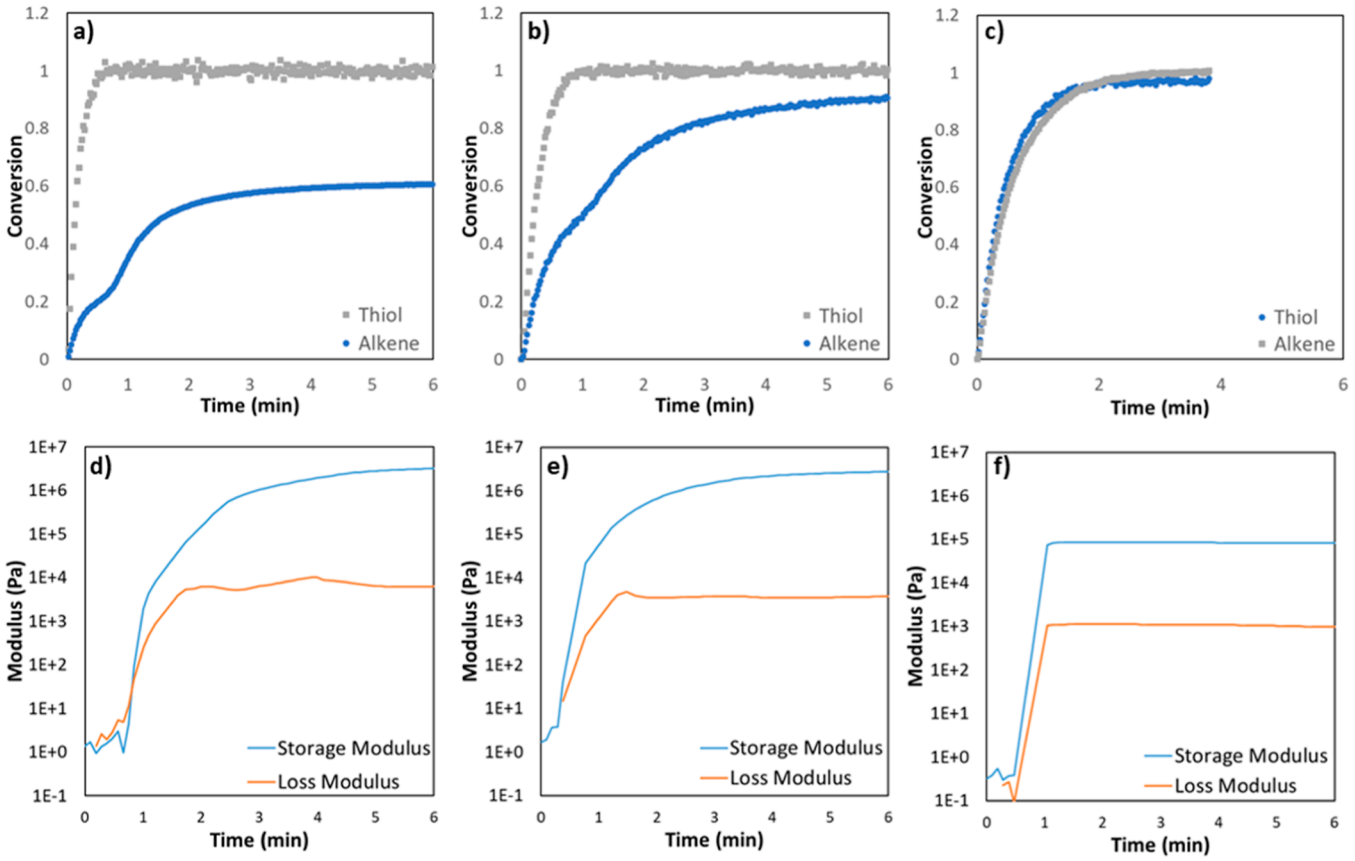


**Figure 7.** Rheometry data obtained from different stoichiometric formulations of DSDVE and PETMP with 1.5 wt % TPO irradiated at 405 nm at an intensity of 14 mW/cm$^2$. (a) Functional group conversion measured by IR *vs* time for a 0.25:1 stoichiometric equivalence of thiol/alkene. (b) IR plot of a 0.5:1 stoichiometric equivalence of thiol/alkene. (c) IR plot of a 1:1 stoichiometric equivalence of thiol/alkene. (d) Storage and loss moduli as measured rheometry as a function of time for a 0.25:1 stoichiometric equivalence of thiol/alkene. (e) Rheometry plot of a 0.5:1 stoichiometric equivalence of thiol/alkene. (f) Rheometry plot of a 1:1 stoichiometric equivalence of thiol/alkene. Figure 7a,d shows a 0.25:1 ratio of thiol to alkene, Figure 7b,e shows a 0.5:1 ratio of thiol to alkene, and Figure 7c,f shows a 1:1 ratio of thiol to alkene.

cross-linking, which may aid in explaining the discrepancy between the results presented herein and those reported in similar systems.

It should be noted that these comparisons with these three by two network polymer systems rely on assumptions regarding the order and arrangement of reacted species that are most likely imperfectly reflective of the reality of DSDVE polymerization. This analogy, however, does lend support to and does not preclude the gelation of this material. For a more in-depth investigation of the heterofunctional Flory−Stockmayer characterization, Tiemersma-Thoone *et al.* present a detailed study.[42]

**Co-polymerizations with PETMP.** Finally, co-polymerization of the DSDVE monomer with PETMP to form insoluble cross-linked networks was investigated. The same three stoichiometric ratios between the monomer and PETMP were tested as in the model studies, and rheology data and functional group conversion data were obtained (Figure 7). Rapid gelation of the material for each stoichiometric formulation of DSDVE and PETMP was achieved upon photoinitiation.

The disulfidation reaction results in twice the number of cross-links compared to the thiol−ene reaction. Therefore, the formulations in which the alkene is consumed by the disulfide−ene reaction result in a nearly 100-fold increase in the storage modulus of the two formulations for which alkenes are available to react with disulfides following the thiol−ene reaction (0.25:1 and 0.5:1) compared to the 1:1 network where thiol−ene is the primary cross-linking reaction.

It was originally hypothesized, and subsequently demonstrated by the model compound kinetics, that the thiol−ene reaction being sufficiently faster than the disulfide−ene reaction would allow for sequential and selective thiol and disulfide consumption to result in a two-step photopolymerization process. For example, the irradiation time can be used to control which polymerization chemistry occurs, where thiol−ene chemistry would proceed to completion in stage I before any significant amount of disulfidation reaction has a chance to occur (stage II). To test this hypothesis, a mixture of PETMP


https://doi.org/10.1021/acs.macromol.1c02464
Macromolecules 2022, 55, 1811−1821

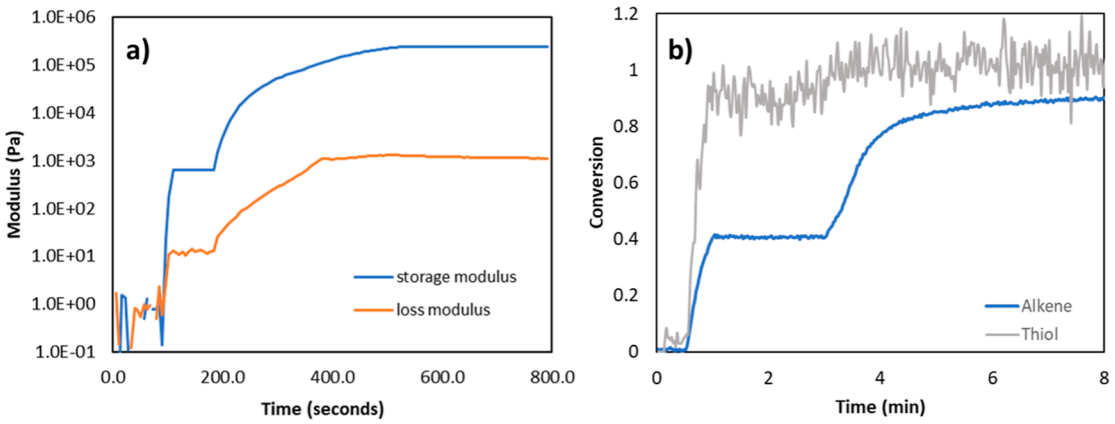


**Figure 8.** Samples prepared with DSDVE and PETMP (1:0.5 alkene/thiol stoichiometric equivalence) with 3 wt % TPO irradiated at 405 nm at 7 mW/cm$^2$. (a) Storage and loss moduli as measured rheometry as a function of time demonstrating control over the storage modulus of the formulated network by controlling the irradiation time. Light is turned on for 30 s, demonstrating near-immediate gelation, primarily *via* thiol−ene chemistry, before the irradiation is stopped. After about 3 min, light is turned back on and storage modulus continues to increase due to the start of disulfidation chemistry. (b) Functional group conversion measured by IR *vs* time demonstrating the time point at which thiol reaches 100% conversion (after roughly 10 s of light exposure), and irradiation is stopped for 2 min. After 3 min, light is turned back on, and alkene consumption continues *via* disulfidation.

and DSDVE (stoichiometry of 0.5:1 thiol/alkene) was irradiated at 7 mW/cm$^2$ for 30 s. The thiol and alkene conversions were measured by IR (Figure 8a), yielding nearly complete conversion of thiols with minimal consumption of the disulfides. Following the initial curing, a second, prolonged irradiation at 7 mW/cm$^2$ facilitated the disulfide−ene reaction. Figure 8b demonstrates that these temporally resolved reactions enable a dual-cure with control over cross-linking density where the thiol−ene polymerization goes to completion after stage 1 curing and can be halted by turning off irradiation, and the disulfidation polymerization proceeds once a stage 2 curing of the disulfides begins. The second stage curing process increases the storage modulus by 2−3 orders of magnitude under these conditions.

This dual-cure system enables controlled manipulation of material properties allowing for a broader scope of potential applications for this polymerization. Figure 9 demonstrates the glass-transition temperatures ($T_g$) corresponding to the first and second stage polymerizations, with an increase of 18 °C between the first stage ($T_{g1}$ = −36 °C) and second stage ($T_{g2}$ = −18 °C). In addition, the high sulfur content in these polymeric systems is an attractive means to obtain materials with useful optical properties. This disulfidation reaction provides an excellent means to achieve such materials. Similar to many thiol−ene-based networks, the material is optically clear in the visible light region after both curing stages.

Finally, a stage I film (same material as in Figure 9) was exposed to UV light through a photomask to create stage II optical index gradient patterns, as illustrated in Figure 10. The photopatterned features, generated as a result of a refractive index change between exposed and unexposed regions, are micrometer-sized squares of high-modulus, high refractive index materials surrounded in a continuous way by a low-modulus stage I matrix. As seen in the microscopic images, good feature resolution is achieved, even at relatively long exposure times (5 min) with noncollimated light. It is argued here that such an outcome was possible uniquely due to the nature of the system at hand where almost all functional groups capable of reacting are tethered to the initial stage I network and therefore immobilized prior to further reaction. Re-

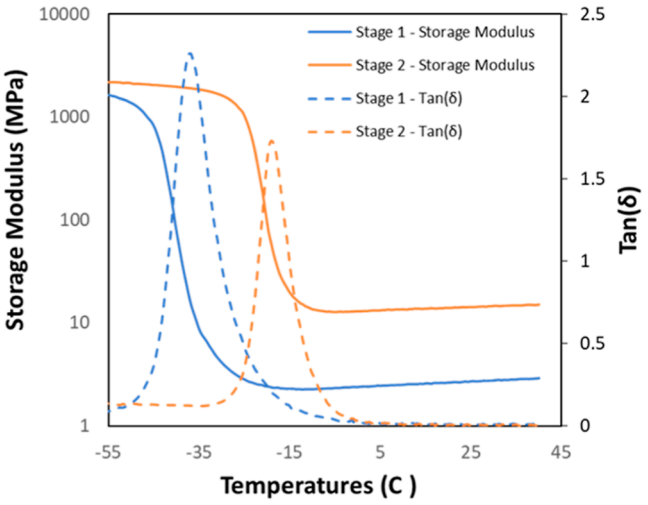


**Figure 9.** Materials consisted of PETMP and DSDVE (0.5:1 thiol/alkene stoichiometric ratio) and 3 wt % TPO. Samples were cast between glass plates with 250 $\mu$m spacers. Samples were irradiated at 405 nm at 14 mW/cm$^2$ for 45 s for the first stage cure and an additional 5 min for the second stage cure.

exposure in a lithographic setup breaks the disulfide cross-links locally in the exposed areas, promoting an area-limited local reactivity increase and thiyl−vinyl coupling, leading to the formation of two thioether links out of one disulfide. Overall, a spatiallyrestricted increase in cross-linking is achieved as well as an increase in refractive index.

## CONCLUSIONS

In summary, a monomer was designed and synthesized that enables sequential photo-induced thiol−ene and disulfide−ene chemistries with appreciable rates and high overall conversions, yielding materials with a high overall sulfur content. The relative rates of the thiol−ene and disulfidation chemistries were investigated, and it was found that the thiol−ene reaction is on average approximately 30 times faster than the disulfidation reaction. This difference in rates enables spatial and temporal control over the two different chemistries


https://doi.org/10.1021/acs.macromol.1c02464
Macromolecules 2022, 55, 1811−1821

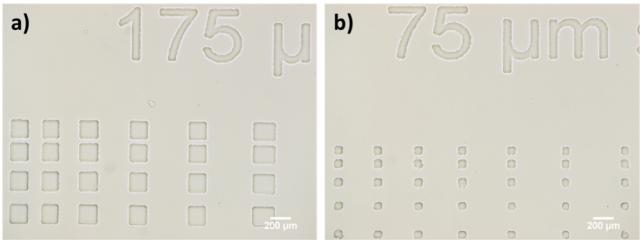


**Figure 10.** Materials consisted of PETMP and DSDVE (0.5:1 thiol/alkene stoichiometric ratio) and 3 wt % TPO. Samples were cast between glass plates with 250 $\mu$m spacers and irradiated with 405 nm light at 14 mW/cm$^2$ for 45 s for the first stage cure and an additional 5 min for the second stage cure. The photopatterned features are a result of a refractive index change between exposed and unexposed regions. (a) After initial UV exposure to form the cross-linked network, a secondary illumination through a photomask produced 175 $\mu$M feature patterns. (b) After an initial UV exposure to form the cross-linked network, a second illumination through a photomask produced 75 $\mu$M feature patterns.

allowing for a dual-cure system. The successful implementation of a two-stage photocure allows a remarkable degree of control of developing material properties, both mechanical and optical. This work provides a new route to high sulfur-containing materials and increases the scope and utility of thiol−X- and disulfide-based polymerizations.

## ■ ASSOCIATED CONTENT

### Supporting Information

The Supporting Information is available free of charge at https://pubs.acs.org/doi/10.1021/acs.macromol.1c02464.

Additional experimental procedures (materials; synthesis protocols; NMR spectroscopy, and FTIR) and corresponding figures (PDF)

## ■ AUTHOR INFORMATION


### Corresponding Author

**Christopher N. Bowman** − *Department of Chemical and Biological Engineering, University of Colorado-Boulder, Boulder, Colorado 80303, United States;* orcid.org/0000-0001-8458-7723; Email: christopher.bowman@colorado.edu

### Authors

**Shafer M. Soars** − *Department of Chemistry, University of Colorado-Boulder, Boulder, Colorado 80303, United States*

**Nicholas J. Bongiardina** − *Materials Science and Engineering Program, University of Colorado-Boulder, Boulder, Colorado 80303, United States*

**Benjamin D. Fairbanks** − *Department of Chemical and Biological Engineering, University of Colorado-Boulder, Boulder, Colorado 80303, United States*

**Maciej Podgórski** − *Department of Chemical and Biological Engineering, University of Colorado-Boulder, Boulder, Colorado 80303, United States; Department of Polymer Chemistry, Institute of Chemical Sciences, Faculty of Chemistry, Maria Curie-Sklodowska University, Lublin 20-031, Poland*

Complete contact information is available at: https://pubs.acs.org/10.1021/acs.macromol.1c02464

### Author Contributions

⊥S.S. and N.B. contributed significantly


### Notes

The authors declare no competing financial interest.

## ■ ACKNOWLEDGMENTS

We gratefully acknowledge financial support from the DARPA grant (W911NF1920024), an NSF grant (1808484), and the US NIH grant (1 F31DE027861-01A1) that made this research possible.

## ■ REFERENCES


(1) Mutlu, H.; Ceper, E. B.; Li, X.; Yang, J.; Dong, W.; Ozmen, M. M.; Theato, P. Sulfur Chemistry in Polymer and Materials Science. *Macromol. Rapid Commun.* **2019**, *40*, No. e1800650.

(2) Kausar, A.; Zulfiqar, S.; Sarwar, M. I. Recent Developments in Sulfur-Containing Polymers. *Polym. Rev.* **2014**, *54*, 185−267.

(3) Boyd, D. A. Sulfur and Its Role In Modern Materials Science. *Angew. Chem. Int. Ed.* **2016**, *55*, 15486−15502.

(4) Martin, R.; Rekondo, A.; de Luzuriaga, A. R.; Casuso, P.; Dupin, D.; Cabañero, G.; Grande, H. J.; Odriozola, I. Dynamic Sulfur Chemistry as a Key Tool in the Design of Self-Healing Polymers. *Smart Mater. Struct.* **2016**, *25*, 084017.

(5) Hoyle, C. E.; Lowe, A. B.; Bowman, C. N. Thiol-Click Chemistry: A Multifaceted Toolbox for Small Molecule and Polymer Synthesis. *Chem. Soc. Rev.* **2010**, *39*, 1355−1387.

(6) Fairbanks, B. D.; Love, D. M.; Bowman, C. N. Efficient Polymer-Polymer Conjugation via Thiol-Ene Click Reaction. *Macromol. Chem. Phys.* **2017**, *218*, 1700073.

(7) Northrop, B. H.; Coffey, R. N. Thiol-Ene Click Chemistry: Computational and Kinetic Analysis of the Influence of Alkene Functionality. *J. Am. Chem. Soc.* **2012**, *134*, 13804−13817.

(8) Lowe, A. B.; Hoyle, C. E.; Bowman, C. N. Thiol-Yne Click Chemistry: A Powerful and Versatile Methodology for Materials Synthesis. *J. Mater. Chem.* **2010**, *20*, 4745−4750.

(9) Cramer, N. B.; Davies, T.; O'Brien, A. K.; Bowman, C. N. Mechanism and Modeling of a Thiol-Ene Photopolymerization. *Macromolecules* **2003**, *36*, 4631−4636.

(10) Long, K. F.; Bongiardina, N. J.; Mayordomo, P.; Olin, M. J.; Ortega, A. D.; Bowman, C. N. Effects of 1°, 2°, and 3° Thiols on Thiol-Ene Reactions: Polymerization Kinetics and Mechanical Behavior. *Macromolecules* **2020**, *53*, 5805−5815.

(11) Goethals, F.; Frank, D.; Du Prez, F. Protected Thiol Strategies in Macromolecular Design. *Prog. Polym. Sci.* **2017**, *64*, 76−113.

(12) Pepels, M.; Filot, I.; Klumperman, B.; Goossens, H. Self-Healing Systems Based on Disulfide-Thiol Exchange Reactions. *Polym. Chem.* **2013**, *4*, 4955−4965.

(13) Bang, E.-K.; Lista, M.; Sforazzini, G.; Sakai, N.; Matile, S. Poly(Disulfide)S. *Chem. Sci.* **2012**, *3*, 1752−1763.

(14) Fang, J.; Ye, S.-H.; Wang, J.; Zhao, T.; Mo, X.; Wagner, W. R. Thiol Click Modification of Cyclic Disulfide Containing Biodegradable Polyurethane Urea Elastomers. *Biomacromolecules* **2015**, *16*, 1622−1633.

(15) Gething, M.-J.; Sambrook, J. Protein Folding in the Cell. *Nature* **1992**, *355*, 33−45.

(16) Rowan, S. J.; Cantrill, S. J.; Cousins, G. R. L.; Sanders, J. K. M.; Stoddart, J. F. Dynamic Covalent Chemistry. *Angew. Chem., Int. Ed.* **2002**, *41*, 898−952.

(17) Saito, G.; Swanson, J. A.; Lee, K.-D. Drug Delivery Strategy Utilizing Conjugation via Reversible Disulfide Linkages : Role and Site of Cellular Reducing Activities. *Adv. Drug Deliv. Rev.* **2003**, *55*, 199−215.

(18) Wojtecki, R. J.; Meador, M. A.; Rowan, S. J. Using the Dynamic Bond to Access Macroscopically Responsive Structurally Dynamic Polymers. *Nat. Mater.* **2011**, *10*, 14−27.

(19) Meng, F.; Hennink, W. E.; Zhong, Z. Biomaterials Reduction-Sensitive Polymers and Bioconjugates for Biomedical Applications. *Biomaterials* **2009**, *30*, 2180−2198.
(20) Gilbert, H. F. Thiol/Disulfide Exchange Equilibria and Disulfidebond Stability. *Methods Enzymol.* **1995**, *251*, 8−28.
(21) Chen, W.; Shah, L. A.; Yuan, L.; Siddiq, M.; Hu, J.; Yang, D. Polymer−Paclitaxel Conjugates Based on Disulfide Linkers for Controlled Drug Release. *R. Soc. Chem.* **2015**, *5*, 7559−7566.
(22) Endo, K.; Murata, K.; Otsu, T. Living Radical Polymerization of Styrene with Tetramethylene Disulfide. *Macromolecules* **1992**, *25*, 5554−5556.
(23) Endo, K.; Shiroi, T.; Murata, K. Controlled Radical Polymerization of Styrene in the Presence of Cyclic 1,2-Disulfides. *J. Polym. Sci., Part A: Polym. Chem.* **2001**, *39*, 145−151.
(24) Chen, J.; Jiang, S.; Gao, Y.; Sun, F. Reducing Volumetric Shrinkage of Photopolymerizable Materials Using Reversible Disulfide-Bond Reactions. *J. Mater. Sci.* **2018**, *53*, 16169−16181.
(25) Barcan, G. A.; Zhang, X.; Waymouth, R. M. Structurally Dynamic Hydrogels Derived from 1,2-Dithiolanes. *J. Am. Chem. Soc.* **2015**, *137*, 5650−5653.
(26) Singh, R.; Whitesides, G. M. Degenerate Intermolecular Thiolate-Disulfide Interchange Involving Cyclic Five-Membered Disulfides Is Faster by ∼10$\hat{3}$ Than That Involving Six- or Seven-Membered Disulfides. *J. Am. Chem. Soc.* **1990**, *112*, 6304−6309.
(27) Tong, C.; Wondergem, J. A. J.; Heinrich, D.; Kieltyka, R. E. Photopatternable, Branched Polymer Hydrogels Based on Linear Macromonomers for 3D Cell Culture Applications. *ACS Macro Lett.* **2020**, *9*, 882−888.
(28) Fernandes, P. A.; Ramos, M. J. Theoretical Insights into the Mechanism for Thiol/Disulfide Exchange. *Chem. Eur J.* **2004**, *10*, 257−266.
(29) Carmine, A.; Domoto, Y.; Sakai, N.; Matile, S. Comparison of Lipoic and Asparagusic Acid for Surface-Initiated Disulfide-Exchange Polymerization. *Chem.—Eur J.* **2013**, *19*, 11558−11563.
(30) Fairbanks, B. D.; Singh, S. P.; Bowman, C. N.; Anseth, K. S. Photodegradable, Photoadaptable Hydrogels via Radical-Mediated Disulfide Fragmentation Reaction. *Macromolecules* **2011**, *44*, 2444−2450.
(31) Mavila, S.; Sinha, J.; Hu, Y.; Podgórski, M.; Shah, P. K.; Bowman, C. N. High Refractive Index Photopolymers by Thiol − Yne " Click " Polymerization. *ACS Appl. Mater. Interfaces* **2021**, *13*, 15647−15658.
(32) Wang, X.-R.; Chen, F. Iodine-Catalyzed Disulfidation of Alkenes. *Tetrahedron* **2011**, *67*, 4547−4551.
(33) Bowman, C. N.; Kloxin, C. J. Toward an Enhanced Understanding and Implementation of Photopolymerization Reactions. *AIChE J.* **2008**, *54*, 2775−2795.
(34) Usugi, S.; Yorimitsu, H.; Shinokubo, H.; Oshima, K. Disulfidation of Alkynes and Alkenes with Gallium Trichloride. *Org. Lett.* **2004**, *5*, 6−8.
(35) Caserio, M. C.; Fisher, C. L.; Kim, J. K. Boron Trifluoride Catalyzed Addition of Disulfides to Alkenes. *J. Org. Chem.* **1985**, *50*, 4390−4393.
(36) Kamps, J.; Soars, S.; Fairbanks, B.; Bowman, C. N. Photodisulfidation of Alkenes with Linear Disulfides: Reaction Scope and Kinetics; *Tetrahedron* [Online early access]. DOI: 10.1016/j.tet.2022.132683. Published Online: Feb 12, **2022**, http://doi.org/10.1016/j.tet.2022.132683.
(37) Cramer, N. B.; Reddy, S. K.; O'Brien, A. K.; Bowman, C. N. Thiol−Ene Photopolymerization Mechanism and Rate Limiting Step Changes for Various Vinyl Functional Group Chemistries. *Macromolecules* **2003**, *36*, 7964−7969.
(38) Neumann, M. G.; Miranda, W. G.; Schmitt, C. C.; Rueggeberg, F. A.; Correa, I. C. Molar Extinction Coefficients and the Photon Absorption Efficiency of Dental Photoinitiators and Light Curing Units. *J. Dent.* **2005**, *33*, 525−532.
(39) Hoyle, C. E.; Lee, T. Y.; Roper, T. Thiol−Enes: Chemistry of the Past with Promise for the Future. *J. Polym. Sci., Part A: Polym. Chem.* **2004**, *42*, 5301−5338.
(40) Konkolewicz, D.; Gray-Weale, A.; Perrier, S. Hyperbranched Polymers by Thiol-Yne Chemistry: From Small Molecules to Functional Polymers. *J. Am. Chem. Soc.* **2009**, *131*, 18075−18077.
(41) Odian, G. *Principles of Polymerization*; 4th ed.; John Wiley & Sons, Inc., 2004.
(42) Tiemersma-Thoone, G. P. J. M.; Scholtens, B. J. R.; Dušek, K.; Gordon, M. Theories for Network Formation in Multistage Processes. *J. Polym. Sci., Part B: Polym. Phys.* **1991**, *29*, 463−482.




https://doi.org/10.1021/acs.macromol.1c02464
*Macromolecules* 2022, 55, 1811−1821